Bulgarian Journal of Physics vol. **49** (2022) 89–96

$N = 90$ Shape Phase Transition: Increasing Axial Asymmetry Towards ^{148}Ce

P. Koseoglou, V. Werner, N. Pietralla

Institut für Kernphysik, Technische Universität Darmstadt, 64289 Darmstadt, Germany

Received *30 November 2021*
doi: https://doi.org/10.55318/bgjp.2022.49.1.089

Abstract. In this proceedings the increasing axial asymmetry in the $N = 90$ isotopes with decreasing atomic number from ^{152}Sm to ^{148}Ce is shown. The placement of the nuclei of interest into the Interacting Boson Model symmetry triangle and the calculations of the approximate effective γ deformation shows the existence of some axial asymmetry, $\gamma_{\text{eff}}^{\text{appr}} \approx 10°$, in ^{148}Ce, while the $N = 90$ ^{152}Sm does not show any. Moreover, the shape evolution study of the cerium, neodymium and samarium chains shows the over all increasing axially asymmetry with decreasing atomic number.

KEY WORDS: Shape phase transition, $N = 90$, cerium isotopic chain, ^{148}Ce, γ degree of freedom, approximate effective γ deformation.

1 The $N = 90$ shape phase transition

Both theoretical and experimental studies have been done on the $N = 90$ shape phase transition (PT) region the last two decades. Some of these studies can be found in Refs. [1–14]. Several symmetries and models describing nuclei in this region have been developed. Nuclei in the critical point of the shape PT between spherical vibrators and well-deformed rigid-rotors can be described by the X(5) symmetry [11]. Analytic solutions of the geometrical Bohr-Hamiltonian can describe nuclei in the spherical side of the phase transition, like the X(5)-β^{2n} models [12], and in the deformed side, like the CBS rotor model [4]. The potentials of each of the models can be seen in red in Figure 1. The X(5)-β^{2n} potential corresponds in the harmonic oscillator for $n = 1$. For increasing n the potential approaches the square well of X(5). The X(5) square well potential approximates the degeneration of the deformed and spherical minima [13]. It describes nuclei on the critical point of the PT. The CBS potential for $\beta_{\text{min}} = 0$ corresponds in the square well potential of X(5). For $\beta_{\text{min}} \approx \beta_{\text{max}}$ the potential approaches the δ function potential of the SU(3) symmetry.

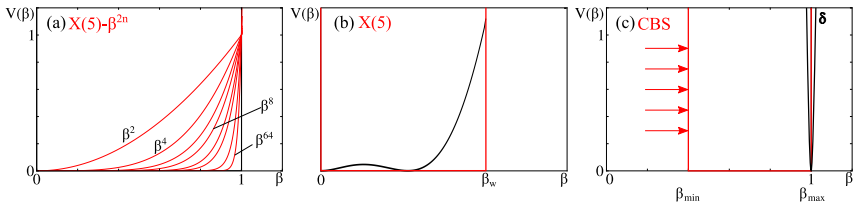

Figure 1. (Color online) β potentials of symmetries describing nuclei on the U(5) to SU(3) leg of the symmetry triangle, in red. (a) The X(5)-β^{2n} potentials. (b) The X(5) square well potential. The black curve shows the two minima in the energy potential surface, the spherical and the deformed, emerging from the IBM-1 Hamiltonian [15]. (c) The CBS potential.

The transition on the N=90 region is obvious in key experimental observables in the gadolinium, samarium, neodymium and cerium isotopes. In particular both the energy ratios, $R_{4/2} = E(4_1^+)/E(2_1^+)$, and the transition strength ratios, $B_{4/2} = B(E2; 4_1^+ \rightarrow 2_1^+)/B(E2; 2_1^+ \rightarrow 0_1^+)$, of the $N = 90$ isotopes show the transitional character of the nuclei. This transition is shown to be more pronounced in samarium and gadolinium, less in neodymium and even less in cerium [16]. See Figure 2. The $R_{4/2}$ values on $N = 88$ are closer to the spherical value 2, specially for gadolinium and samarium isotopes, while on the $N = 90$ the values are close to the transitional value 2.9, emerging from the X(5) symmetry.

The above mentioned symmetry and models describe axially symmetric nuclei, with $\gamma = 0°$. In Figure 3 the low-energy spectra of the $N = 90$ nuclei are shown together with the values emerging from the X(5) model. All isotopes seems to be close to the X(5) symmetry. The position of the band-head of the γ-band (the 2_γ^+ state) for each isotope, with respect to the ground-band, is shown with

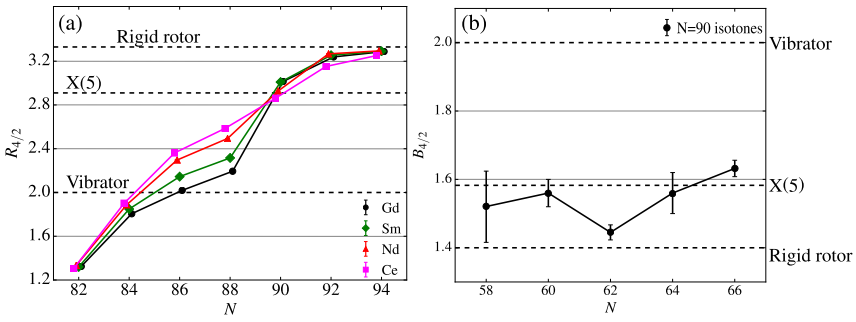

Figure 2. (Color online) (a) $R_{4/2}$ ratios for Gd, Sm, Nd and Ce isotopic chains. The values are taken from [17]. (b) $B_{4/2}$ ratios for the $N = 90$ isotones. All values are taken from [17], beside for ^{148}Ce which is taken from [10].

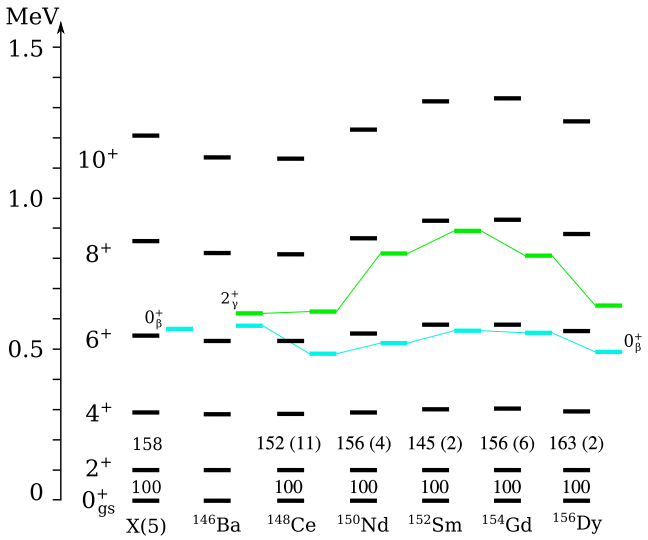

Figure 3. (Color online) Energy spectra of the N=90 isotones and the X(5) symmetry. The energies of the levels of each isotope are normalized to the energy of the 2_1^+ state which is shifted to 100 keV. The 0_2^+ states are plotted with blue and the 2_γ^+ states are plotted with green. The $B(E2)$ values presented are normalized at $B(E2; 2_1^+ \rightarrow 0_1^+) = 100$. The $B(E2)$ values are taken from [17], beside for ^{148}Ce which is taken from [10].

green. One can see that the trend of the 2_γ^+ states shows increasing γ degree of freedom as one moves away from ^{152}Sm. This raises the need of considering the γ degree of freedom in the comparison of the experimental data with the models, as the atomic number decreases from samarium to cerium. The entire transitional region can be mapped within the algebraic Interacting Boson Model (IBM)-1 [18, 19], considering also axially-asymmetric nuclei.

2 IBM-1 Calculations

In the framework of the IBM Arima and Iachello describe collective excitations of nuclei in terms of bosons as pairs of valence fermions [20]. The IBM has been proven, for the first time in the samarium isotopic chain [21], to be able to describe the collective properties of nuclei with a large range of structures. The ζ and χ are used as structural parameters in the IBM. The symmetry triangle can be mapped with $\zeta \in [0, 1]$ and $\chi \in [-\sqrt{7}/2, 0]$ parameters (see Figure 4). Larger χ values indicate the higher γ-asymmetry, as one approach the O(6) symmetry, which describes γ-soft nuclei. The method described in Refs. [19,22] was followed in order to place the nuclei of interest into the symmetry triangle by comparing the IBM-1 calculations with the experimental data. In the present work the IBM-1 calculations were performed in the whole IBM symmetry tri-

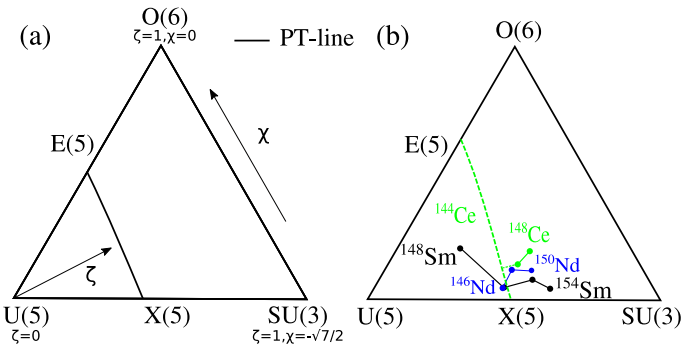

Figure 4. (Color online) (a) The IBM symmetry triangle. (b) Placement of the samarium, neodymium and cerium isotopic chains into the IBM symmetry triangle. Adapted from Ref. [10].

angle using the IBAR code [23]. The full description of the specific calculations can be found in Refs. [10, 24].

The placement of the samarium, neodymium and cerium isotopic chains into the symmetry triangle can be seen in Figure 4. The ζ and χ parameters for each isotope can be seen in Table 1. Since the 0_2^+ state is not experimentally known for ^{144}Ce, the nucleus can not be placed into the triangle in one point. Instead

Table 1. Coordinates of isotopes in the symmetry triangle. *The placement of ^{144}Ce in one spot was not possible because the energy of the 0_2^+ state is not experimentally known. The isotope was placed in an area instead, using the energy ratio $R_{4/2}$. The $\gamma_{\rm eff}^{\rm appr}$, calculated from the $K_3^{\rm appr}$ parameter, is given for each isotope. The $N = 90$ isotones are in "bold" for easier comparison.

Isotope	ζ	χ	$\gamma_{\rm eff}^{\rm appr}$
^{146}Ba	**0.69**	**-0.78**	**12°**
^{144}Ce*	0.5 to 0.6	0 to $-\sqrt{7}/2$	
^{146}Ce	0.59	-1.02	10°
^{148}Ce	**0.64**	**-0.94**	**9°**
^{146}Nd	0.50	-1.17	12°
^{148}Nd	0.56	-1.04	14°
^{150}Nd	**0.62**	**-1.08**	**5°**
^{148}Sm	0.43	-0.68	23°
^{150}Sm	0.51	-1.14	11°
^{152}Sm	**0.61**	**-1.13**	**1°**
^{154}Sm	0.65	-1.23	3°
^{154}Gd	**0.63**	**-0.93**	**7°**
^{156}Dy	**0.62**	**-0.87**	**8°**

the $R_{4/2}$ ratio was used to place it along a line [10]. One can see the increasing γ asymmetry along the cerium isotopic chain, by increasing neutron number. The cerium isotopic chain is heading far from the base of the triangle, towards the center of the triangle where higher γ asymmetry is expected. While the neodymium and the samarium chains (more for samarium) stay near the base of the triangle, indicating the low γ asymmetry of the isotopes.

3 Approximate Effective γ Deformation

In order to quantify the γ asymmetry, the approximate effective γ deformation ($\gamma_{\text{eff}}^{\text{appr}}$) can be calculated from the cubic shape parameter K_3. Once the nucleus is placed in the symmetry triangle, the ζ and χ coordinates are defined, the IBM-1 calculation can provide a large number of observables. In particular the B(E2) transition strengths can be used in order to gain information for the shape of the nucleus. The quadrupole shape invariants [25–27], introduced by Kumar are model independent and direct observables related to the shape of a nucleus. The cubic shape parameter K_3 [28], which is derived from the q_2 and q_3 shape invariants, is related to the γ degree of freedom. In Ref. [29] it was shown that K_3 can be obtained with good accuracy, with $K_3 \approx K_3^{\text{appr}}$. The K_3^{appr} is given from the equation

$$K_3^{\text{appr}} = \sqrt{\frac{7}{10}}\,\text{sign}\,(Q(2_1^+))\left[\sqrt{\frac{B(E2;2_1^+ \to 2_1^+)}{B(E2;2_1^+ \to 0_1^+)}} - 2\frac{\sqrt{B(E2;2_2^+ \to 0_1^+)B(E2;2_2^+ \to 2_1^+)}}{B(E2;2_1^+ \to 0_1^+)}\right], \quad (1)$$

where $B(E2;2_1^+ \to 2_1^+)$ is given from the quadrupole moment $Q(2_1^+)$,

$$B(E2;2_1^+ \to 2_1^+) = \frac{35}{32\pi}Q(2_1^+)^2. \quad (2)$$

The $\gamma_{\text{eff}}^{\text{appr}}$ in the ground state is possible to derive from the K_3^{appr}. Note, that one talks of effective γ deformation, since the nucleus does not have a rigid γ-softness. The $\gamma_{\text{eff}}^{\text{appr}}$ derives from

$$K_3^{\text{appr}} = -\cos(3\gamma_{\text{eff}}^{\text{appr}}). \quad (3)$$

The differences between the exact $\gamma_{eff.}$ and the approximate $\gamma_{\text{eff}}^{\text{appr}}$ were shown not to excess the 2.5° [29] for $N_B = 10$ and any ζ, χ combination. One should expect the case to be the same for $N_B = 7$–12, which correspond to the values used for the calculations performed in this work.

The $\gamma_{\text{eff}}^{\text{appr}}$ calculated from the equations above and the IBM-1 calculations for each isotope of interest are given in Table 1. The values are also plotted in

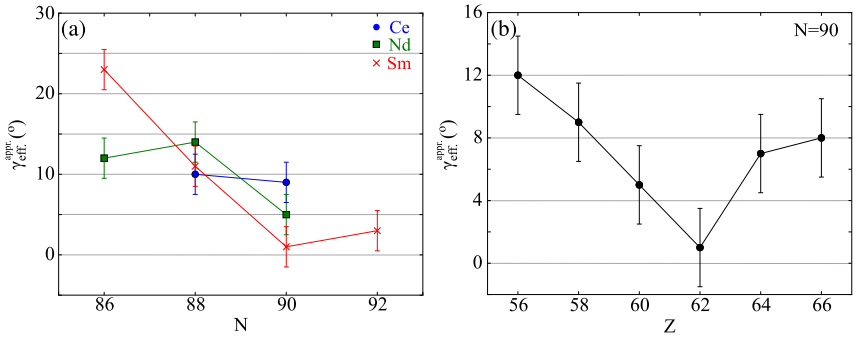

Figure 5. (Color online) The calculated $\gamma_{\text{eff}}^{\text{appr}}$ for (a) the cerium, neodymium and samarium isotopic chains and (b) for the $N = 90$ isotones. Adapted from Ref. [24].

Figure 5. For both ^{146,148}Ce isotopes the $\gamma_{\text{eff}}^{\text{appr}} \approx 10°$, shows the existence of some γ asymmetry. While the $\gamma_{\text{eff}}^{\text{appr}}$ values calculated for the samarium isotopes show a drastic decrease of the axial asymmetry for increasing neutron number from $N = 86$ to $N = 90$. The near to zero value for ^{152}Sm explains the good description of the isotope by the CBS model which considers the γ-part of the nuclear potential as an harmonic oscillator (potential minimum at $\gamma = 0°$) [4]. For neodymium the $\gamma_{\text{eff}}^{\text{appr}}$ values show the same picture as for samarium isotopic chain. The $\gamma_{\text{eff}}^{\text{appr}}$ values show a drastic decrease of the axial asymmetry for increasing atomic number from $Z = 56$ to $Z = 62$ for the $N = 90$ isotones.

4 Conclusions

The axial asymmetry in the samarium, neodymium and cerium isotopic chains near the $N = 90$ region were investigated within the IBM-1 and quantified through the approximate effective γ deformation. The increased axial asymmetry in the cerium isotopic chain, in comparison with the samarium and the neodymium isotopic chains, was shown. As it was shown in Ref. [10] this increased axial asymmetry plays an important role in the comparison with the geometrical symmetries and the placement of ^{148}Ce in the deformed side of the symmetry triangle. This picture was also supported by microscopic calculations for the isotope. More, in Refs. [16, 24] axial asymmetry in the cerium isotopic chain was associated with the less pronounced shape PT.

Acknowledgements

P.K. was supported by the Research Cluster ELEMENTS, the LOEWE research funding program of the state of Hesse and by the Bulgarian National Science Fund (BNSF) contract number KP-06-N28/6. This work was also supported by the HGS-HIRe for FAIR and the NuSTAR.DA BMBF 05P(15/19)RDFN1.

References

[1] R.F. Casten, N.V. Zamfir (2001) Empirical Realization of a Critical Point Description in Atomic Nuclei. *Phys. Rev. Lett.* **87** 052503. DOI: https://doi.org/10.1103/PhysRevLett.87.052503.

[2] D. Warner (2002) A triple point in nuclei. *Nature* **420** 614. DOI: https://doi.org/10.1038/420614a.

[3] R.F. Casten (2006) Shape phase transitions and critical-point phenomena in atomic nuclei. *Nat. Phys.* **2** 811. DOI: https://doi.org/10.1038/nphys451.

[4] N. Pietralla, O.M. Gorbachenko (2004) Evolution of the "β excitation" in axially symmetric transitional nuclei. *Phys. Rev. C* **70** 011304(R). DOI: https://doi.org/10.1103/PhysRevC.70.011304.

[5] R. Krücken et al. (2002) B(E2) Values in ^{150}Nd and the Critical Point Symmetry X(5). *Phys. Rev. Lett.* **88** 232501. DOI: https://doi.org/10.1103/PhysRevLett.88.232501.

[6] D. Tonev et al. (2004) Transition probabilities in ^{154}Gd: Evidence for X(5) critical point symmetry. *Phys. Rev. C* **69** 034334. DOI: https://doi.org/10.1103/PhysRevLett.88.232501.

[7] T. Nikšić et al. (2007) Microscopic Description of Nuclear Quantum Phase Transitions. *Phys. Rev. Lett.* **99** 092502. DOI: https://doi.org/10.1103/PhysRevLett.99.092502.

[8] Z.P. Li et al. (2009) Microscopic analysis of nuclear quantum phase transitions in the N≈90 region. *Phys. Rev. C* **79** 054301. DOI: https://doi.org/10.1103/PhysRevC.79.054301.

[9] J. Wiederhold et al. (2016) Fast-timing lifetime measurement of ^{152}Gd. *Phys. Rev. C* **94** 044302. DOI: https://doi.org/10.1103/PhysRevC.94.044302.

[10] P. Koseoglou et al. (2020) Low-Z boundary of the N = 88-90 shape phase transition: ^{148}Ce near the critical point. *Phys. Rev. C* **101** 014303. DOI: https://doi.org/10.1103/PhysRevC.101.014303.

[11] F. Iachello (2000) Dynamic Symmetries at the Critical Point. *Phys. Rev. Lett.* **85** 3580. DOI: https://doi.org/10.1103/PhysRevLett.85.3580.

[12] D. Bonatsos et al. (2004) Sequence of potentials interpolating between the U(5) and E(5) symmetries. *Phys. Rev. C* **69** 044316. DOI: https://doi.org/10.1103/PhysRevC.69.044316.

[13] F. Iachello (2001) Analytic Description of Critical Point Nuclei in a Spherical-Axially Deformed Shape Phase Transition. *Phys. Rev. Lett.* **87** 052502. DOI: https://doi.org/10.1103/PhysRevLett.87.052502.

[14] E. Williams et al. (2010) Effective critical points in finite quantum phase transitional systems. *Phys. Rev. C* **82** 054308. DOI: https://doi.org/10.1103/PhysRevC.82.054308.

[15] P. Van Isacker, Jin-Quan Chen (1981) Classical limit of the interacting boson Hamiltonian. *Phys. Rev. C* **24** 684–689. DOI: http://dx.doi.org/10.1103/PhysRevC.24.684.

[16] P. Koseoglou et al. (2019) $N = 90$ QSPT: Cerium, neodymium and samarium isotopic chains in the IBM symmetry triangle. In: *Proceedings of the HNPS2018, the 27th Annual Symposium of the Hellenic Nuclear Physics Society* **0,2018**.

[17] ENSDF database (accessed 11.2021) available at http://www.nndc.bnl.gov/.

[18] F. Iachello, A. Arima (1987) "*The Interacting Boson Approximation Model*". Cambridge University Press, Cambridge.

[19] E.A. McCutchan et al. (2004) Mapping the interacting boson approximation symmetry triangle: New trajectories of structural evolution of rare-earth nuclei. *Phys. Rev. C* **69** 064306. DOI: https://doi.org/10.1103/PhysRevC.69.064306.

[20] A. Arima, F. Iachello (1975) Collective Nuclear States as Representations of a SU(6) Group. *Phys. Rev. Lett.* **35** 1069.
DOI: https://doi.org/10.1103/PhysRevLett.35.1069.

[21] O. Scholten et al. (1978) Interacting boson model of collective nuclear states III. The transition from SU(5) to SU(3). *Annals Phys.* **115** 2.
DOI: https://doi.org/10.1016/0003-4916(78)90159-8.

[22] E.A. McCutchan, R.F. Casten (2006) Crossing contours in the interacting boson approximation (IBA) symmetry triangle. *Phys. Rev. C* **74** 057302.
DOI: https://doi.org/10.1103/PhysRevC.74.057302.

[23] R.J. Casperson (2012) IBAR: Interacting boson model calculations for large system sizes. *Comp. Phys. Comm.* **183** 4.
DOI: http://dx.doi.org/https://doi.org/10.1016/j.cpc.2011.12.024.

[24] P. Koseoglou (2019) Lifetime measurements in the neutron-rich ^{148}Ce nuclide at the low-Z boundary of the N=90 shape-phase transition. PhD thesis. Darmstadt: Technische Universität. DOI: http://tuprints.ulb.tu-darmstadt.de/8592/.

[25] Krishna Kumar (1972) Intrinsic Quadrupole Moments and Shapes of Nuclear Ground States and Excited States. *Phys. Rev. Lett.* **28** 249.
DOI: https://doi.org/10.1103/PhysRevLett.28.249.

[26] D. Cline (1986) Nuclear Shapes Studied by Coulomb Excitation. *Annu. Rev. Nucl. Part. Sci.* **36.1** 683–716.
DOI: http://dx.doi.org/10.1146/annurev.ns.36.120186.003343.

[27] R.V. Jolos et al. (1997) Shape invariants in the multiple "Q-excitation" scheme. *Nucl. Phys. A* **618** 1.
DOI: http://dx.doi.org/https://doi.org/10.1016/S0375-9474(97)00046-8.

[28] V. Werner et al. (2000) Quadrupole shape invariants in the interacting boson model. *Phys. Rev. C* **61** 021301(R). DOI: https://doi.org/10.1103/PhysRevC.61.021301.

[29] V. Werner et al. (2005) Triaxiality and the determination of the cubic shape parameter K_3 from five observables. *Phys. Rev. C* **71** 054314.
DOI: http://dx.doi.org/10.1103/PhysRevC.71.054314.